

Orientation Dependence of Epitaxial and One-Axis-Oriented (Ba_{0.5}Sr_{0.5})TiO₃ Films Prepared by RF Magnetron Sputtering

Sinichi ITO*, Kenji TAKAHASHI, Shoji OKAMOTO, Ivoyl P. KOUTSAROFF¹,
Andrew CERVIN-LAWRY¹ and Hiroshi FUNAKUBO

Department of Innovative and Engineered Materials, Tokyo Institute of Technology,
G1-405, 4259 Nagatsuta-Cho, Midori-Ku, Yokohama 226-8502, Japan

¹Technology R&D, Genuum Corporation, 970 Fraser Drive, Burlington, Ontario L7L 5P5, Canada

(Received May 28, 2005; accepted June 24, 2005; published September 22, 2005)

The dependences of electrical properties on (111) and (100) orientations were investigated for (Ba_{0.5}Sr_{0.5})TiO₃ films with in-plane random (one-axis-oriented films) and aligned orientations (epitaxial films) prepared by RF magnetron sputtering. Epitaxial films with (100) and (111) orientations were grown on (100)_cSrRuO₃//(100)SrTiO₃ and (111)_cSrRuO₃//(111)SrTiO₃ substrates, while one-axis-oriented films were grown on (100)_cSrRuO₃/(100)_cLaNiO₃/(111)Pt/TiO₂/SiO₂/Al₂O₃ and (111)_cSrRuO₃/(111)Pt/TiO₂/SiO₂/Al₂O₃ substrates, respectively. Films with the (111) orientation had larger relative dielectric constants, ϵ_r , measured at an oscillation of 20 mV and 100 kHz under an applied dc bias electric field of 0 kV/cm and a larger tunability against the dc bias electric field than (100)-oriented films for both epitaxial and one-axis orientations. These data show the dependences of ϵ_r and tunability on orientation were existed, irrespective of the in-plane orientation and the thermal strain caused in the film by the substrates. [DOI: 10.1143/JJAP.44.6881]

KEYWORDS: epitaxial film, one-axis oriented film, (Ba,Sr)TiO₃, BST, orientation dependence, dielectric properties, RF magnetron sputtering, Al₂O₃ ceramic substrate

1. Introductions

(Ba_{0.5}Sr_{0.5})TiO₃ (BST) has been widely investigated in tunable microwave devices such as phase shifters, delay lines, resonators, tunable filters, and varactors due to its high relative dielectric constant (ϵ_r), tunability and low dielectric loss ($\tan \delta$).¹⁾ The BST ceramic system has a phase transition from a paraelectric cubic phase to a ferroelectric tetragonal phase and has a maximum in relative dielectric constant–temperature plots. In the case of thin film BST, the maximum in the ϵ_r [$\epsilon_{\max}(T)$] has been suppressed and has shown a very broad temperature dependence accompanied with a temperature shift of $\epsilon_{\max}(T)$.²⁾

In capacitance–dc bias electric field (C – E) characteristics, a butterfly-shaped curve typically appearing in ferroelectric materials was frequently observed for paraelectric BST films.³⁾ This suggests the contribution of the ferroelectricity in the film. This also shows the possibility that ϵ_r has an orientation dependence and that its tunability may be similar to that observed for ferroelectric BST thin films.⁴⁾ In fact, the orientation dependences of the dielectric property at zero dc bias electric field was reported for (100)-, (110)- and (111)-oriented BST films grown on (100), (110) and (111) MgO substrates, respectively.⁵⁾ However, the effect of an in-plane orientation in epitaxial BST films as reported by Moon *et al.*⁵⁾ was not made clear, even though for practical applications of BST films only non-epitaxial films, either randomly oriented or one-axis-oriented films, can be used. In addition, a dependence of ϵ_r on orientation for films deposited on Si^{2,6)} or Al₂O₃⁷⁾ substrates has not been reported, in spite of the fact that the ϵ_r and tunability of the BST film is known to be strongly affected by strain from the substrate.^{8,9)} Moreover, the thermal strain applied to the film, the dominant strain from the substrate, deposited on Si and Al₂O₃ substrates is opposite that of the BST films deposited on MgO substrates.

In this study, we first investigated the electrical properties of (100)- and (111)-oriented epitaxial BST films grown on SrRuO₃-coated SrTiO₃ substrates. In addition, we compare the results for the same out-of-plane-oriented films with those for in-plane randomly oriented (or one-axis-oriented) films deposited on Al₂O₃ ceramic substrates. On the basis of these results, we discuss the dielectric anisotropy of the films, taking into account the effect of in-plane orientation and the strain from the substrates on these properties.

2. Experimental

BST films 210 nm thick were deposited at 800°C by RF magnetron sputtering. Film thickness was ascertained using a field emission–scanning electron microscope (FE-SEM) with cross-sectional observation. The total gas pressure was 1.0×10 Pa under an Ar/O₂ gas ratio of 9/1. The films obtained were annealed at 500°C in atmospheric O₂ flow for 30 min. Epitaxial SrRuO₃ films 100 nm thick were deposited on (100) and (111) SrTiO₃ single crystals at 750°C by metal organic chemical vapor deposition (MOCVD), and (100)_cSrRuO₃//(100)SrTiO₃ and (111)_cSrRuO₃//(111)-SrTiO₃ shown in Figs. 1(a) and 1(b) were used as substrates for growing epitaxial BST film. A pseudo-cubic Miller index designated as $(hkl)_c$ was used for SrRuO₃^{10–12)} as well as for LaNiO₃. On the other hand, the stacks of (100)_cSrRuO₃/(100)_cLaNiO₃/(111)Pt/TiO₂/SiO₂/Al₂O₃ and (111)_cSrRuO₃/(111)Pt/TiO₂/SiO₂/Al₂O₃ shown in Figs. 1(c) and 1(d) were used as substrates to prepare one-axis-oriented BST film. The details of the preparation of Pt/TiO₂/SiO₂/Al₂O₃ and the upper buffer layers have been reported elsewhere.^{7,13)}

The crystal structure of the films was characterized by X-ray diffraction (XRD). The composition of the films was ascertained using a wavelength dispersion X-ray fluorescence (XRF) spectrometer. The electrical properties of Pt/BST/SrRuO₃ capacitors were characterized after making Pt top electrodes by electron-beam evaporation on BST films through dots 100 μm in diameter using a shadow mask.

*E-mail address: funakubo@iem.titech.ac.jp

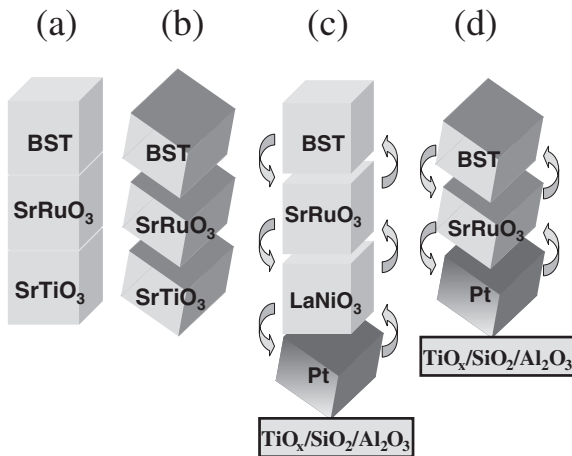


Fig. 1. Schematic models of epitaxial BST films [(a) and (b)] and one-axis-oriented BST films [(c) and (d)]. (a) BST/(100)_cSrRuO₃/(100)-SrTiO₃. (b) BST/(111)_cSrRuO₃/(111)SrTiO₃. (c) BST/(100)_cSrRuO₃/(100)_cLaNiO₃/(111)Pt/TiO₂/SiO₂/Al₂O₃. (d) BST/(111)_cSrRuO₃/(111)Pt/TiO₂/SiO₂/Al₂O₃.

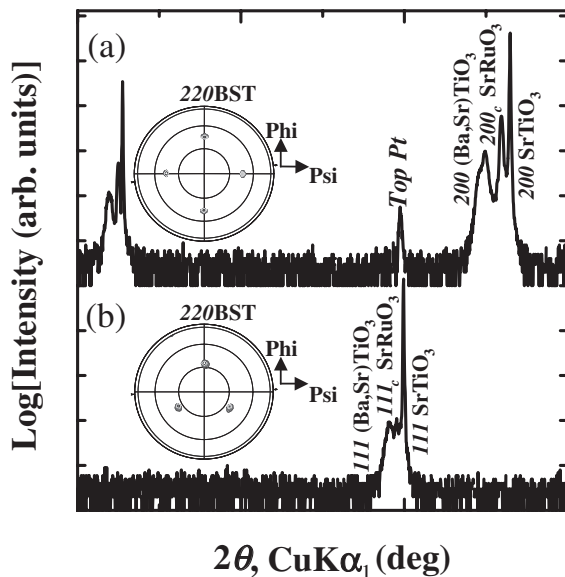


Fig. 2. X-ray diffraction patterns and X-ray pole-figure plots fixed at 2θ position corresponding to 220BST. (a) BST/(100)_cSrRuO₃/(100)-SrTiO₃. (b) BST/(111)_cSrRuO₃/(111)SrTiO₃.

Capacitance–dc bias electric field (C – E) characteristics with an oscillation at 20 mV and 100 kHz were measured using an HP 4194A. Tunability was measured under an applied dc bias electric field and was defined as $[\varepsilon_r(0 \text{ kV/cm}) - \varepsilon_r(E_{\text{max}})]/\varepsilon_r(0)$ (%), where $\varepsilon_r(0 \text{ kV/cm})$ and $\varepsilon_r(E_{\text{max}})$ correspond to ε_r at 0 kV/cm and E_{max} kV/cm, respectively.

3. Results and Discussion

3.1 Epitaxial BST films

Figure 2 shows the θ – 2θ XRD and the X-ray pole-figure plots fixed at the 2θ position corresponding to 220BST for the films grown on (100)_cSrRuO₃/(100)SrTiO₃ and (111)_cSrRuO₃/(111)SrTiO₃ substrates. Only (100) and (200) diffraction peaks of BST films were verified on θ – 2θ XRD patterns for the films grown on (100)_cSrRuO₃/(100)SrTiO₃ substrates and (111) peaks for those on

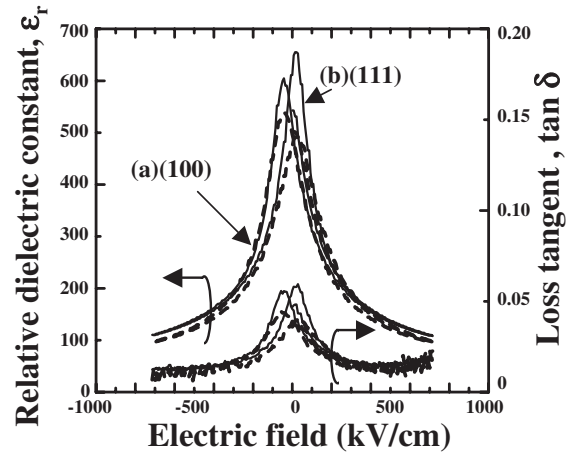


Fig. 3. Relative dielectric constant (ε_r) and loss tangent ($\tan\delta$) as functions of applied dc bias electric field for the same films as shown in Fig. 2. (a) BST/(100)_cSrRuO₃/(100)SrTiO₃ (dotted line). (b) BST/(111)_cSrRuO₃/(111)SrTiO₃ (solid line).

(111)_cSrRuO₃/(111)SrTiO₃ substrates. In addition, four and three concentrated poles located at $\psi = 45$ and 35° were observed in pole-figure plots as shown in the insets of Figs. 2(a) and 2(b), respectively. These data show that (100)- and (111)-oriented BST films were ascertained to be epitaxially grown on (100)_cSrRuO₃/(100)SrTiO₃ and (111)_cSrRuO₃/(111)SrTiO₃ substrates, respectively.

Figure 3 shows the change in ε_r and $\tan\delta$ as functions of the dc bias electric field for the same BST films shown in Fig. 2. The ε_r of the (111)-oriented BST film was larger than that of the (100)-oriented film, particularly in the low dc bias electric field region, but the ε_r at a high dc bias electric field was almost the same for both films. This suggests that the change in ε_r with dc bias electric field (also known as tunability) of the (111)-oriented BST film was larger than that of the (100)-oriented film. It must be mentioned that the tunability in $\tan\delta$ of the (111)-oriented film was also larger than that of the (100)-oriented film. The tunabilities for the dc bias electric fields up to an E_{max} of 250 kV/cm and 700 kV/cm were 61.3% and 81.8% for (100)-oriented film, respectively and 66.6% and 83.3% for (111)-oriented BST film, respectively.

3.2 One-axis-oriented BST films

To clarify the effect of the strain applied to the BST film from the substrate and the in-plane orientation, (100)- and (111)-oriented films with an in-plane random orientation were deposited on Al₂O₃ substrates, the thermal expansion coefficient (α_{TEC}) of which was smaller than that of the BST film, while that of the SrTiO₃ substrate was larger than that of the BST film.

Figure 4 shows the XRD patterns and the X-ray pole-figure plots fixed at the 2θ position corresponding to 220BST for the films deposited on (100)_cSrRuO₃/(100)_cLaNiO₃/(111)Pt/TiO₂/SiO₂/Al₂O₃ and (111)_cSrRuO₃/(111)Pt/TiO₂/SiO₂/Al₂O₃ substrates. Only (100) and (200) diffraction peaks were verified on θ – 2θ XRD patterns for the BST films grown on (100)_cSrRuO₃/(100)_cLaNiO₃/(111)Pt/TiO₂/SiO₂/Al₂O₃ substrates, and a (111) peak in the case of (111)_cSrRuO₃/(111)Pt/TiO₂/SiO₂/Al₂O₃ substrates, just

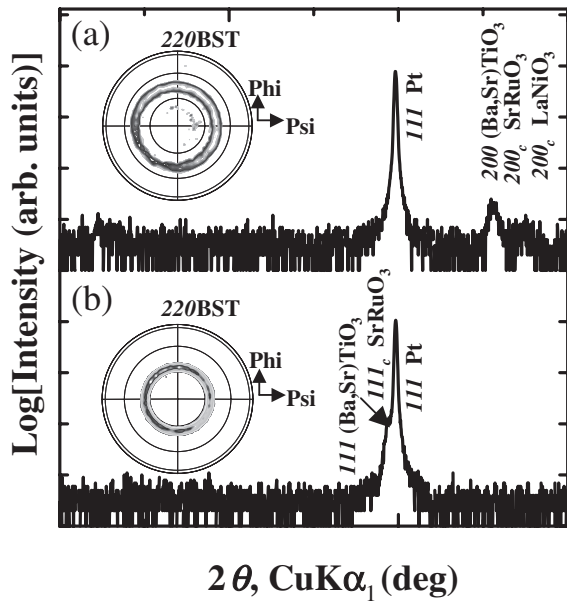


Fig. 4. X-ray diffraction patterns and pole figure plots fixed at 2θ position corresponding to 220BST . (a) $\text{BST}/(100)_c\text{SrRuO}_3/(100)_c\text{LaNiO}_3/(111)\text{Pt}/\text{TiO}_2/\text{SiO}_2/\text{Al}_2\text{O}_3$. (b) $\text{BST}/(111)_c\text{SrRuO}_3/(111)\text{Pt}/\text{TiO}_2/\text{SiO}_2/\text{Al}_2\text{O}_3$.

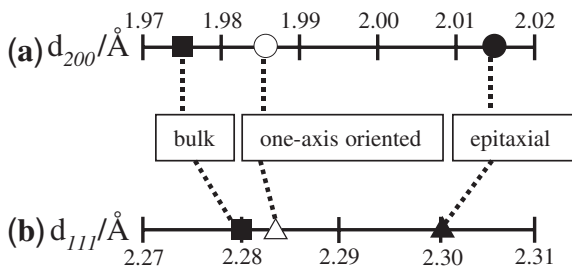


Fig. 5. Lattice spacings of (a) d_{200} and (b) d_{111} estimated from epitaxial and one-axis-oriented BST films shown in Figs. 2 and 4 for (100)- and (111)-oriented films, respectively. (●): $\text{BST}/(100)_c\text{SrRuO}_3/(100)\text{SrTiO}_3$. (▲): $\text{BST}/(111)_c\text{SrRuO}_3/(111)\text{SrTiO}_3$. (○): $\text{BST}/(100)_c\text{SrRuO}_3/(100)_c\text{LaNiO}_3/(111)\text{Pt}/\text{TiO}_2/\text{SiO}_2/\text{Al}_2\text{O}_3$. (△): $\text{BST}/(111)_c\text{SrRuO}_3/(111)\text{Pt}/\text{TiO}_2/\text{SiO}_2/\text{Al}_2\text{O}_3$. (□): reported data for bulk $(\text{Ba}_{0.5}\text{Sr}_{0.5})\text{TiO}_3$.

as was the case for BST films grown on $(100)_c\text{SrRuO}_3/(100)\text{SrTiO}_3$ and $(111)_c\text{SrRuO}_3/(111)\text{SrTiO}_3$ substrates. However, ringed poles located at $\psi = 45$ and 35° were observed on X-ray pole-figure plots as shown in the insets of Figs. 4(a) and 4(b), respectively. These data show that (100) and (111) one-axis-oriented BST films with an in-plane random orientation were prepared on $(100)_c\text{SrRuO}_3/(100)_c\text{LaNiO}_3/(111)\text{Pt}/\text{TiO}_2/\text{SiO}_2/\text{Al}_2\text{O}_3$ and $(111)_c\text{SrRuO}_3/(111)\text{Pt}/\text{TiO}_2/\text{SiO}_2/\text{Al}_2\text{O}_3$ substrates, respectively.

Figure 5 summarizes the lattice spacing of 200BST and 111BST obtained from 200BST and 111BST diffraction peaks, d_{200} and d_{111} , respectively, for the (100) and (111)-oriented films shown in Figs. 2 and 4. Epitaxial BST films have larger d_{200} and d_{111} values than one-axis-oriented films. This implies the possibility that epitaxial films are in a more highly compressed state than one-axis-oriented films along the in-plane orientation. However, both epitaxial and one-axis-oriented BST films have larger d_{200} and d_{111} values than those reported for bulk BST with the same Ba/Sr ratio.

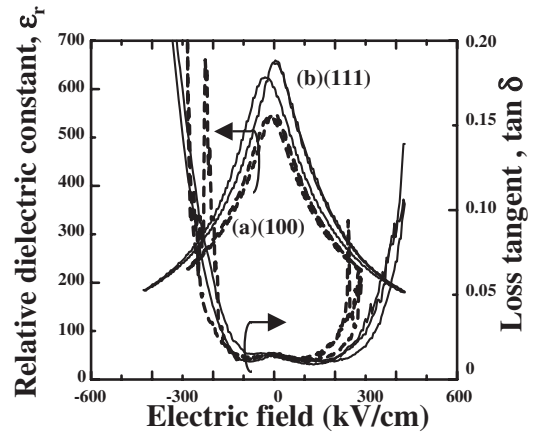


Fig. 6. ϵ_r and $\tan \delta$ as functions of applied dc bias electric field for the same BST films as shown in Fig. 4. (a) $\text{BST}/(100)_c\text{SrRuO}_3/(100)_c\text{LaNiO}_3/(111)\text{Pt}/\text{TiO}_2/\text{SiO}_2/\text{Al}_2\text{O}_3$ (dotted line). (b) $\text{BST}/(111)_c\text{SrRuO}_3/(111)\text{Pt}/\text{TiO}_2/\text{SiO}_2/\text{Al}_2\text{O}_3$ (solid line).

There is a possibility that a larger unit cell than that of the bulk BST reported by Abe and Komatsu¹⁴⁾ exists for sputtered films in the $\text{SrTiO}_3\text{-BaTiO}_3$ system.

Figure 6 shows the change in ϵ_r and $\tan \delta$ as a function of the dc bias electric field for the same type of BST films as shown in Fig. 4. The ϵ_r of (111)-oriented BST film was also larger than that of (100)-oriented film at the low dc bias electric field region, but those at the high dc bias electric field were comparable for both BST films and were very similar to the tunabilities of the epitaxial BST films shown in Fig. 3. The dependence of $\tan \delta$ on the applied electric field demonstrated a similar behavior. These data allow us to conclude that the tunabilities in ϵ_r and $\tan \delta$ of (111)-oriented one-axis film were also larger than those of (100)-oriented film. The tunability for dc bias electric fields up to an E_{max} of 250 kV/cm was 55.8 and 59.6% for (100)- and (111)-oriented films, respectively.

3.3 Comparison with dielectric properties of epitaxial and one-axis-oriented films

Figure 7 summarizes the tunability for the dc bias electric fields up to an E_{max} of 250 kV/cm for the (100)- and (111)-oriented BST films. The tunability of the (111)-oriented one-axis film was larger than that of the (100)-oriented film for both films together with the same trend in $\tan \delta$, suggesting crystal anisotropy in the ϵ_r and $\tan \delta$ of BST films. This anisotropy in the dielectric properties of BST films is very similar to the tendency reported at 9 GHz by Moon *et al.*⁵⁾ They pointed out the following three possible reasons: polarization changes come from magnitude variations in the relative displacement of Ti ions with respect to O ions, the domain growth mechanism changes, and the strain and stress changes in perovskite BST films. In this study, a similar anisotropy was ascertained even at a low frequency of 100 kHz. These data suggest that the origin of the anisotropy can be applicable over a wider frequency range. One possibility, the strain and stress changes pointed out by Moon *et al.*, is now under investigation by changing the substrate: Si, MgO and SrTiO_3 . In addition, the crystal anisotropy did not depend on the in-plane orientation and the thermal strain applied to the films from the substrates. These

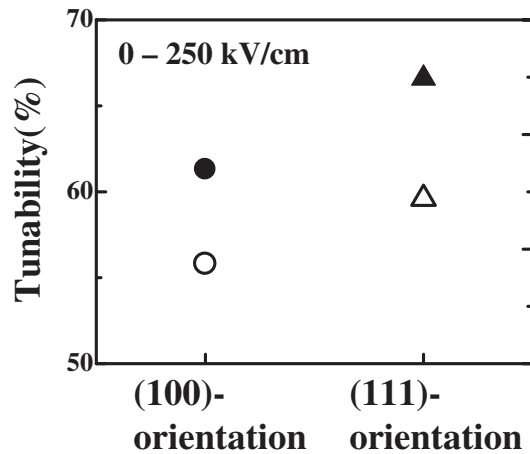


Fig. 7. Tunability for dc bias electric fields up to E_{\max} of 250 kV/cm for epitaxial and one-axis-oriented BST films shown in Figs. 3 and 6 for (100)- and (111)-oriented films. (●): BST// $(100)_c$ SrRuO₃// (100) SrTiO₃. (▲): BST// $(111)_c$ SrRuO₃// (111) SrTiO₃. (○): BST/ $(100)_c$ SrRuO₃/ $(100)_c$ LaNiO₃/ (111) Pt/TiO₂/SiO₂/Al₂O₃. (△): BST/ $(111)_c$ SrRuO₃/ (111) Pt/TiO₂/SiO₂/Al₂O₃.

data suggest that the crystal orientation of BST films engineered on templates used in this study produces a larger ϵ_r near 0 kV/cm dc bias electric fields, and the tunability becomes as high as that for ferroelectric BST films.⁴⁾

4. Conclusions

(100)- and (111)-oriented one-axis and epitaxial BST films were prepared by RF magnetron sputtering. (100)- and (111)-oriented epitaxial films were grown on $(100)_c$ -SrRuO₃// (100) SrTiO₃ and $(111)_c$ SrRuO₃// (111) SrTiO₃ substrates, while (100)- and (111)-oriented one-axis films were grown on $(100)_c$ SrRuO₃/ $(100)_c$ LaNiO₃/ (111) Pt/TiO₂/SiO₂/Al₂O₃ and $(111)_c$ SrRuO₃/ (111) Pt/TiO₂/SiO₂/Al₂O₃

substrates, respectively. A larger ϵ_r near 0 kV/cm and tunability against the dc bias electric field were obtained for (111)-oriented BST films than for (100)-oriented films for both epitaxial and one-axis-oriented films. Crystal structure anisotropy, irrespective of the thermal strain applied to the film and the in-plane orientation, was confirmed for ϵ_r near 0 kV/cm and for the tunability of BST films.

Acknowledgements

We would like to thank Dr. Takehito Jimbo from ULVAC Inc. for his useful discussions.

- 1) M. J. Lancaster, J. Powell and A. Porch: Supercond. Sci. & Technol. **11** (1998) 1323.
- 2) C. Parker, J.-P. Maria and A. Kingon: Appl. Phys. Lett. **81** (2002) 340.
- 3) S. Cha, B. Jang and H. Lee: Jpn. J. Appl. Phys. **38** (1999) L49.
- 4) T. Oikawa, M. Aratani, H. Funakubo, K. Saito and M. Mizuhira: J. Appl. Phys. **95** (2004) 3111.
- 5) S. Moon, E. Kim, M. Kwak, H. Ryu, Y. Kim, K. Kang, S. Lee and W. Kim: Appl. Phys. Lett. **83** (2003) 2166.
- 6) C. Basceri, S. Streiffer, A. Kingon and R. Waser: J. Appl. Phys. **82** (1997) 2497.
- 7) I. P. Koutsaroff, T. Bernacki, M. Zelner, A. Cervin-Lawry, T. Jimbo and K. Suu: Jpn. J. Appl. Phys. **43** (2004) 6740.
- 8) A. Sharma, Z.-G. Ban, S. P. Alpay and J. V. Mantese: Appl. Phys. Lett. **85** (2004) 985.
- 9) T. R. Taylor, P. J. Hansen, B. Acikel, N. Pervez, R. A. York, S. K. Streiffer and J. S. Speck: Appl. Phys. Lett. **80** (2002) 1978.
- 10) K. Takahashi, T. Oikawa, K. Saito, S. Kaneko, H. Fujisawa, M. Shimizu and H. Funakubo: Jpn. J. Appl. Phys. **41** (2002) 5376.
- 11) K. Takahashi, T. Oikawa, K. Saito, H. Fujisawa, M. Shimizu and H. Funakubo: Jpn. J. Appl. Phys. **41** (2002) 6873.
- 12) K. Takahashi, M. Suzuki, T. Oikawa, H. Chen and H. Funakubo: Mater. Res. Soc. Symp. Proc. **833** (2005) G1.9.1.
- 13) S. Okamoto, S. Yokoyama, Y. Honda, G. Asano and H. Funakubo: Jpn. J. Appl. Phys. **43** (2004) 6567.
- 14) K. Abe and S. Komatsu: J. Appl. Phys. **77** (1995) 6461.